

# Characterization of Amorphous Hydrogenated Carbon Formed by Low-Pressure Inductively Coupled Plasma Enhanced Chemical Vapor Deposition Using Multiple Low-Inductance Antenna Units

Osamu Tsuda,<sup>\*,†</sup> Masatou Ishihara,<sup>†</sup> Yoshinori Koga,<sup>†</sup> Shuzo Fujiwara,<sup>‡</sup> Yuichi Setsuhara,<sup>§</sup> and Naoyuki Sato<sup>||</sup>

Research Center for Advanced Carbon Materials, National Institute of Industrial Science and Technology (AIST), Tsukuba Central 5, 1-1-1 Higashi, Tsukuba, Ibaraki, 305-8565, Japan, Research Center for Explosion Safety, National Institute of Industrial Science and Technology (AIST), Tsukuba Central 5, 1-1-1 Higashi, Tsukuba, Ibaraki, 305-8565, Japan, Joining and Welding Research Institute, Osaka University, 11-1 Mihogaoka, Ibaraki, Osaka, 567-0047, Japan, and Institute of Applied Beam Science, Graduate School of Science and Engineering, Ibaraki University, 4-12-1 Nakanarusawa-cho, Hitachi, Ibaraki 316-8511, Japan

Received: October 7, 2004; In Final Form: January 7, 2005

Three-dimensional plasma enhanced chemical vapor deposition (CVD) of hydrogenated amorphous carbon (*a*-C:H) has been demonstrated using a new type high-density volumetric plasma source with multiple low-inductance antenna system. The plasma density in the volume of  $\phi$  200 mm  $\times$  100 mm is  $5.1 \times 10^{10} \text{ cm}^{-3}$  within  $\pm 5\%$  in the lateral directions and  $5.2 \times 10^{10} \text{ cm}^{-3}$  within  $\pm 10\%$  in the axial direction for argon plasma under the pressure of 0.1 Pa and the total power as low as 400 W. The uniformity of the thickness and refractive index is within  $\pm 3.5\%$  and  $\pm 1\%$ , respectively, for the *a*-C:H films deposited on the substrates placed on the six side walls, the top of the  $\phi$  60 mm  $\times$  80 mm hexagonal substrate holder in the pure toluene plasma under the pressure is as low as 0.04 Pa, and the total power is as low as 300 W. It is also found that precisely controlled ion bombardment by pulse biasing led to the explicit observation in Raman and IR spectra of the transition from polymer-like structure to diamond-like structure accompanied by dehydrogenation due to ion bombardment. Moreover, it is also concluded that the pulse biasing technique is effective for stress reduction without a significant degradation of hardness. The stress of 0.6 GPa and the hardness of 15 GPa have been obtained for 2.0  $\mu\text{m}$  thick films deposited with the optimized deposition conditions. The films are durable for the tribology test with a high load of 20 N up to more than 20 000 cycles, showing the specific wear rate and the friction coefficient were  $1.2 \times 10^{-7} \text{ mm}^3/\text{Nm}$  and 0.04, respectively.

## 1. Introduction

Diamondlike carbon (DLC) has been attracting attention in the field of tribology due to its high hardness, low friction, high wear resistance, and excellent chemical inertness.<sup>1–5</sup> For the application to protective coatings against high load tribology environments, such as automotive powertrain components and cutting tools, long lifetime and sufficiently large thickness, which must be of the order of microns, are required as well as the low friction and specific wear rate.<sup>6</sup> The improvement in interface adhesion strength or reduction in internal film stress extends the lifetime of the coatings. Thus deposition process is required for the formation of the films with sufficiently low stress and without the degradation of other properties such as hardness, specific wear rate, friction coefficient, etc. Another requirement for DLC coating is the ability of deposition onto volumetric complex shaped objects. For this purpose, we have developed a plasma-based ion implantation technique using an electron cyclotron resonance (ECR) plasma with a magnetic mirror field for uniform coating of amorphous hydrogenated

carbon (*a*-C:H)<sup>7–10</sup> and demonstrated *a*-C:H deposition on end mills<sup>11</sup> and motorcycle pistons.<sup>12</sup> However, further scaling up of this method is dimensionally restricted by the size of the ECR electromagnets.

Recently, a new type high density inductively coupled plasma (ICP) source without a magnetic field has been developed by Setsuhara et al. using multiple low-inductance rectangular internal antenna units.<sup>13</sup> They have found that only 100 W power input enables the generation of high-density argon plasma of  $4 \times 10^{10} \text{ cm}^{-3}$  at 1.1 Pa with an efficiency as high as 80%. This technique has provided a way to produce uniform plasma in a 1 m sized chamber.

In the present study, we have developed a new type deposition system for *a*-C:H coating onto volumetric objects using low-pressure ICP enhanced CVD method with the multiple low-inductance rectangular internal antenna units. Using this method with pulsed RF biasing technique, we demonstrate three-dimensional coating of *a*-C:H films. Effects of pulsed RF biasing, such as the substrate bias voltage and the duty ratio of the RF pulse voltage, on the structure, internal stress, and mechanical and tribological properties of the deposited films are also investigated for the purpose of survey of the optimized deposition conditions for *a*-C:H coating with low stress, high hardness, low specific wear rate, and long lifetime against wear.

\* Corresponding author. Tel: +81-29-861-4551. Fax: +81-29-851-5425. E-mail: oz.tsuda@aist.go.jp.

<sup>†</sup> Research Center for Advanced Carbon Materials, AIST.

<sup>‡</sup> Research Center for Explosion Safety, AIST.

<sup>§</sup> Osaka University.

<sup>||</sup> Ibaraki University.

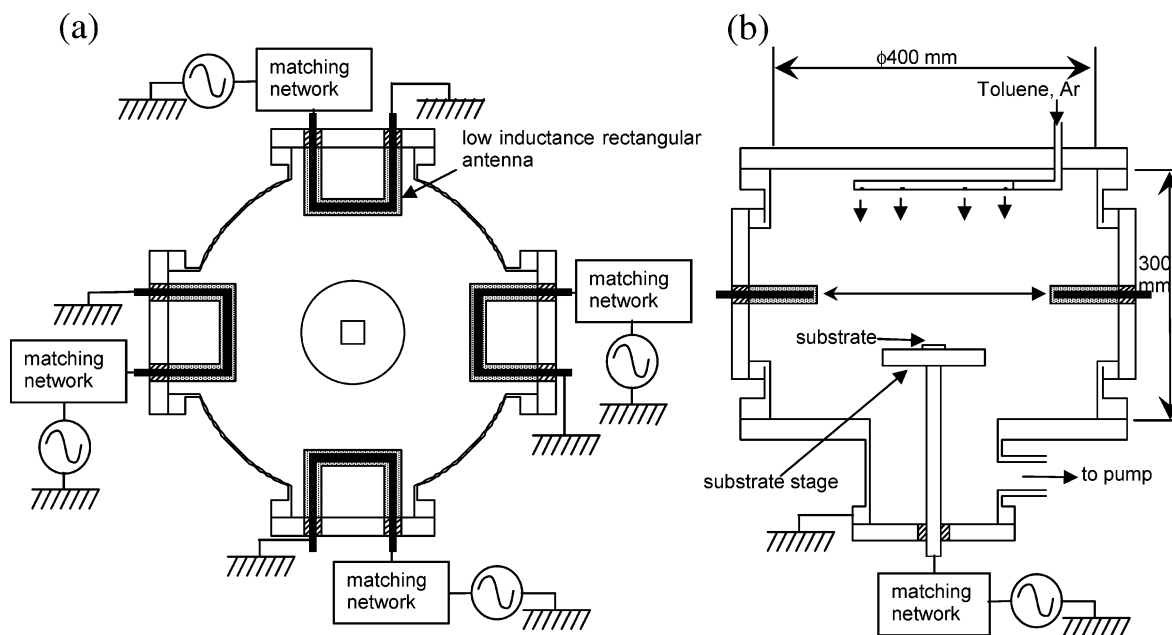


**Figure 1.** Schematic illustration of low-pressure inductively coupled plasma enhanced chemical vapor deposition equipment with low-inductance rectangular multi-antenna system. (a) Top view, (b) side view.

## 2. Experimental Section

The schematic illustration of the apparatus used is shown in Figure 1. The chamber had an inner diameter of 400 mm and a height of 300 mm. Each low-inductance rectangular antenna was a water-cooled 1/4 in. copper tube covered with a quartz insulating tube with a dimension of 100 mm in width and 100 mm in length, and was mounted on an ICP 203 flange. The apparatus has four antennas, which were placed horizontally and evenly in azimuthal direction and were individually and equally excited by four 13.56 MHz RF power sources. The RF voltages applied to the antennas were synchronized by a phase shifting unit to suppress the mutual interference. Negative substrate self-bias voltage ( $V_s$ ) was applied to the substrate electrode by a 13.56 MHz RF generator which could generate RF power in a pulse mode.

The film depositions were performed with a pure toluene plasma at the pressure ( $p$ ) of 0.04 Pa after the chamber was evacuated below  $4 \times 10^{-4}$  Pa, and then the sputter cleaning was made in a pure argon plasma with  $V_s = 100$  V for 10 min. The flow rate of the toluene source gas was 5.6 sccm. The RF power ( $P$ ) was varied from 75 to 100 W. The negative bias voltage was applied to the substrate electrode both in the continuous mode and in the pulse mode. The frequency of the pulsed RF voltage was fixed to be 1 kHz.  $V_s$  and the duty ratio ( $R_d$ ) were varied from floating (no biasing) to 500 V and from 10% (pulse mode) to 100% (continuous mode), respectively. The deposition time was fixed to be 30 min, except for the thicker specimen prepared for 120 min for long-run tribology tests. The film thickness was 500–800 nm for the deposition time of 30 min. Si (100) wafers were used as substrates. The experiments were made with the procedures as follow. First, the survey of the deposition conditions for films with low stress and high hardness was carried out. In this series of experiments, Si substrates were placed on the substrate stage (electrode). Then three-dimensional coating was performed with the optimal conditions using a  $\phi$  60 mm  $\times$  80 mm hexagonal substrate holder. In this experiment, seven substrates were placed on the six side wall and the top of the holder on the substrate stage.

The deposited films were analyzed by Raman spectroscopy (Jasco, model NRS-2100: 514.5 nm Ar ion laser) and IR

absorption spectroscopy (Jasco, model FT/IR-680plus). Mechanical properties of the films were measured with a nanoindentation tester (MTS, model Nanoindenter XP). Internal stress was derived from the curvature of the specimen measured with a surface profilometer (KLA Tencor, model P-15) using Stoney's equation. Measurements of tribological properties were performed by a ball-on-disk system (CSEM, model TRIBOMETER) in a dry air. The balls used were  $\phi$  4 mm silicon carbide. The stroke and the speed were 5 mm and 10 mm/s, respectively. The load and the cycles were set to be 1 N and 7000 cycles, respectively, except for a long-run test where the load was varied from 1 to 20 N, and the cycles was varied from 1000 to 20 000. Thickness measurement was made by cross-sectional observation with scanning electron microscopy (Hitach, model H-2000) and reflectometry (Filmetrics, model F20 system).

Spatial distribution of electron density and electron temperature were measured by a Langmuir probe system which has axial, radial and azimuthal movements. The scanning volume of the Langmuir probe was  $\phi$  200 mm in diameter and 100 mm in height, which was 15 mm distant from the substrate stage.

## 3. Results and Discussions

**3.1. Plasma Diagnostics.** The axial position ( $X$ ), the radial position ( $R$ ) and azimuthal angle ( $\theta$ ) of the probe scanning directions were chosen as shown in Figure 2a. Panels b and c of Figure 2 show the probe electron-saturation current in the axial and lateral directions, respectively. The plasma measured was generated with  $P = 100$  W, where the total input was 400 W, in a pure argon with the pressure from 0.1 to 0.5 Pa. At  $p = 0.50$  Pa, the distribution of the probe electron-saturation current in the axial direction in the center of chamber was within  $\pm 10\%$  for  $X = -70$  to 30 mm (Figure 2b). At reduced pressures, the uniformity in the axial position was improved, and was  $\pm 1.5\%$  when the pressure was reduced to be 0.10 Pa. The averaged electron density in the lateral direction was  $5.1 \times 10^{10} \text{ cm}^{-3}$ . Moreover, in the lateral plane at  $X = 0$ , the probe current was almost uniform within  $\pm 1.5\%$  in the azimuthal direction and  $\pm 5\%$  in the radial direction with  $R = 0$  to 100 mm, respectively (Figure 2c). The probe scanning in the axial direction was limited to the region with the height of 100 mm

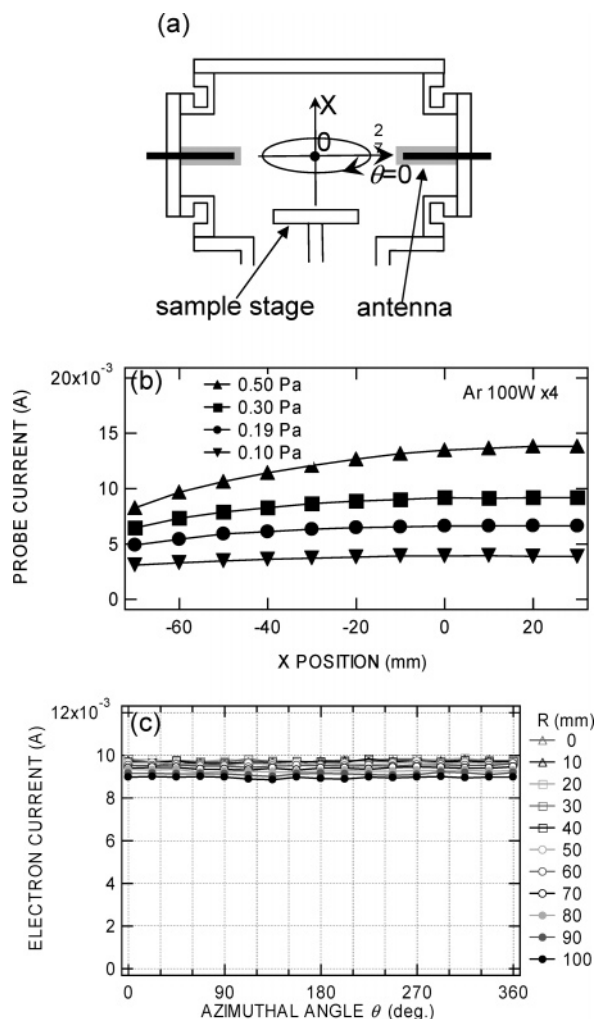


**Figure 2.** (a) Probe scanning directions, (b) axial distributions of the electron saturation current in the center of the chamber with  $p = 0.10$  Pa – 0.50 Pa of argon, and (c) lateral distribution of the electron saturation current in the plane at  $X = 0$  mm with  $p = 0.10$  Pa.

( $X = -70$  to  $30$  mm) by the probe scanning mechanics and the chamber shape. Taking the symmetry of the apparatus into account, the uniformity is considered to be still  $\pm 10\%$  for  $X$  from  $-70$  to  $70$  mm, that is, for the height of  $140$  mm. In this case of  $p = 0.10$  Pa, the averaged electron density in the axial direction was as high as  $5.2 \times 10^{10} \text{ cm}^{-3}$ , and the averaged electron temperature and the averaged plasma potential were  $5.8$  eV and  $33$  V, respectively. The electron density is comparable with those reported in the study with mirror-type ECR plasma enhanced CVD for  $a\text{-C:H}$  deposition.<sup>7</sup> Thus the ICP with the low-inductance antenna system is effective for a more large volumetric plasma generation for CVD of  $a\text{-C:H}$ . Moreover, the pressure as low as  $0.10$  Pa and the electron density as high as  $5.2 \times 10^{10} \text{ cm}^{-3}$  were sufficient for a collisionless sheath formation, indicating that the present method is effectively utilized for CVD with assistance of energetic ion bombardment by DC or RF biasing. Since the uniformity in the axial direction is sufficiently good, it would be improved further in size by piling-up of the antennas in this direction.

**3.2. Characterization of  $a\text{-C:H}$  Films.** **3.2.1. Raman and IR Absorption Measurement.** Panels a, b, and c of Figure 3 show Raman spectra of the  $a\text{-C:H}$  films deposited with  $P_s = 75$  W,  $100$  W and various  $V_s$  with  $R_d = 100\%$ ,  $50\%$ , and  $10\%$ , respectively. The Raman spectrum of the film deposited without the bias voltage has a high background signal and no specific

peak (Figure 3a), showing the formation of polymer-like carbon composed of small rings of aromatic molecules or polyene chains.<sup>14</sup> The films deposited with  $V_s$  equal to or above  $50$  V exhibited a broad peak at  $1530 \text{ cm}^{-1}$  and a shoulder at  $1350 \text{ cm}^{-1}$ , which correspond to the G-band and the D-band of the  $a\text{-C:H}$  which is so-called “diamondlike carbon” (DLC), respectively.<sup>14,15</sup> In the case of  $R_d = 10\%$ , only a high background signal was observed for  $V_s = 50$  V (Figure 3c), indicating the film had a large amount of the polymer-like component. When  $V_s$  was raised from  $50$  to  $500$  V, the Raman spectra were gradually changed from those for the polymer-like films to those for the DLC films similar with  $R_d = 50\%$  or  $100\%$ . The  $V_s$  and  $R_d$  dependence of the Raman spectra shows that energetic ion bombardment enhances the formation of DLC and that the elevated  $V_s$  compensated the reduced  $R_d$ . In one period of the pulse ( $1$  ms) the increase in thickness is only  $3 \times 10^{-4} \text{ nm}$  for the deposition rate of  $20 \text{ nm/min}$ , and is much less than the ion range which is a few monolayer to several nanometers for the ion energy of  $50\text{--}1000 \text{ eV}$ .<sup>16,17</sup> Thus the growing surface was substantially subject to the continuous ion bombardment even with the pulse biasing. Therefore the tradeoff relationship between  $V_s$  and  $R_d$  means that the ion energy and the ion flux complementarily affect the formation of DLC. Moreover it is concluded that precisely controlled ion bombardment by the pulse biasing led to the explicit observation of the transition from the polymer-like structure at  $V_s = 50$  V to the DLC structure  $V_s = 500$  V shown in Figure 3c.

Panels a, b, and c of Figure 4 show IR absorption spectra of the deposited films with  $P = 75$  W,  $100$  W, and various  $V_s$  with  $R_d = 100\%$ ,  $50\%$ , and  $10\%$ , respectively. Each spectrum was shifted vertically for guide-to-eye. For the case of no bias (Figure 4a), the spectrum has an absorption band at  $2923 \text{ cm}^{-1}$  and a shoulder at  $2850 \text{ cm}^{-1}$  which correspond to  $sp^3 \text{ C-H}$  and/or  $\text{C-H}_2$  (asym.) stretching mode(s) and  $sp^3 \text{ C-H}_2$  (sym.) stretching mode, respectively.<sup>18</sup> The spectrum also exhibits a small peak at  $3023 \text{ cm}^{-1}$  originating from olefinic  $sp^2 \text{ C-H}_2$  vibrations. The intensities of these absorption peaks and the shoulder decreased with an increase in  $V_s$ . The relative intensity of the shoulder at  $2850 \text{ cm}^{-1}$  to that of the absorption at  $2923 \text{ cm}^{-1}$  also decreased with increasing  $V_s$ . These spectra changes indicate the structural change from the structure including C-H bonds to that with reduced C-H bonds due to dehydrogenating caused by the energetic ion bombardment.<sup>19</sup> This dependence on  $V_s$  is also found for the case of  $R_d = 50\%$  (Figure 4b), and is especially clear for the case of  $10\%$  (Figure 4c). With decreasing  $R_d$  from  $100\%$  to  $10\%$  (a–c) at the same  $V_s$ , the absorption at  $2923 \text{ cm}^{-1}$  increased. No clear difference in the IR spectra were found between the samples deposited with  $P = 75$  and  $100$  W. These results are consistent with those of the Raman measurement, showing that the structure change from polymer-like carbon to DLC occurs with breaking of bonds between carbon and hydrogen atoms caused by ion bombardment with sufficient energy and flux.

**3.2.2. Internal Stress, Hardness, and Tribological Properties.** Figure 5a shows the dependence of internal compressive stress of the films on  $V_s$  and  $R_d$ . In the case of  $R_d = 100\%$ , the stress had a maximum of  $2.6 \text{ GPa}$  at  $V_s = 200$  V. With decreasing  $R_d$ , the stress was drastically reduced and independent to  $V_s$ . As well as the stress, the hardness also decreased with decreasing  $R_d$  (Figure 5b). However, in contrast to the stress, the hardness of the films increased with  $V_s$  below  $100$  V and was almost constant with  $V_s = 100\text{--}500$  V for  $R_d = 100\%$  and  $P = 100$  W. For  $R_d = 10\%$  and  $50\%$  the hardness monotonically increased with  $V_s$ . These results mean that the pulse biasing

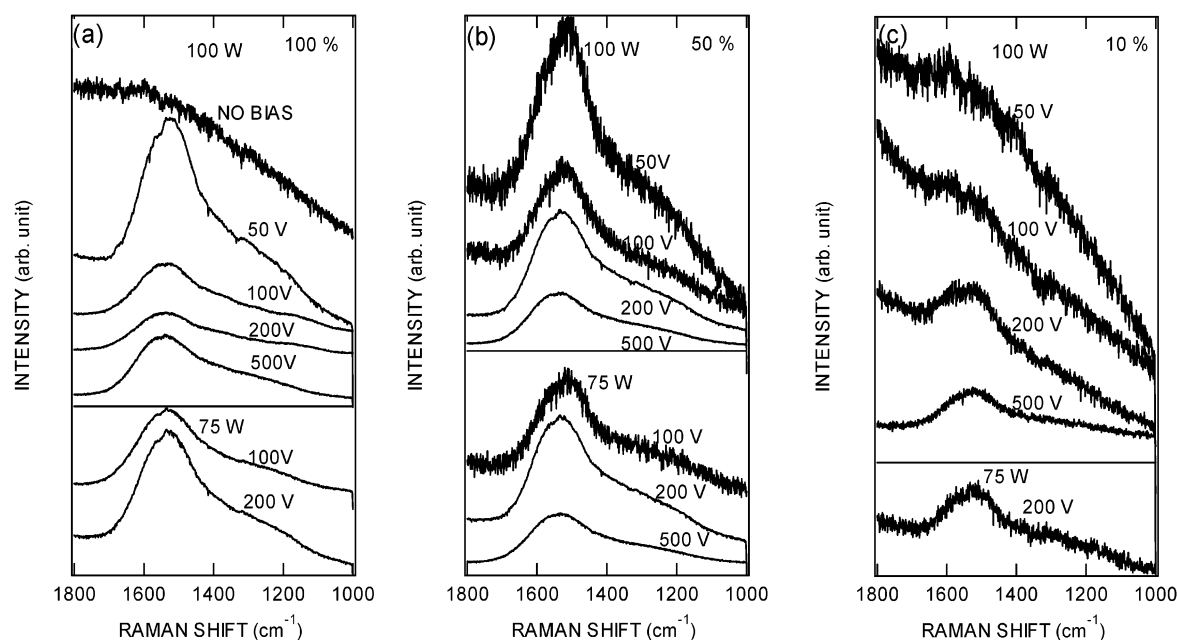


**Figure 3.** Raman spectra of the films deposited with various  $V_s$  at  $P = 75$  and  $100$  W and  $R_d =$  (a) 100%, (b) 50%, and (c) 10%.

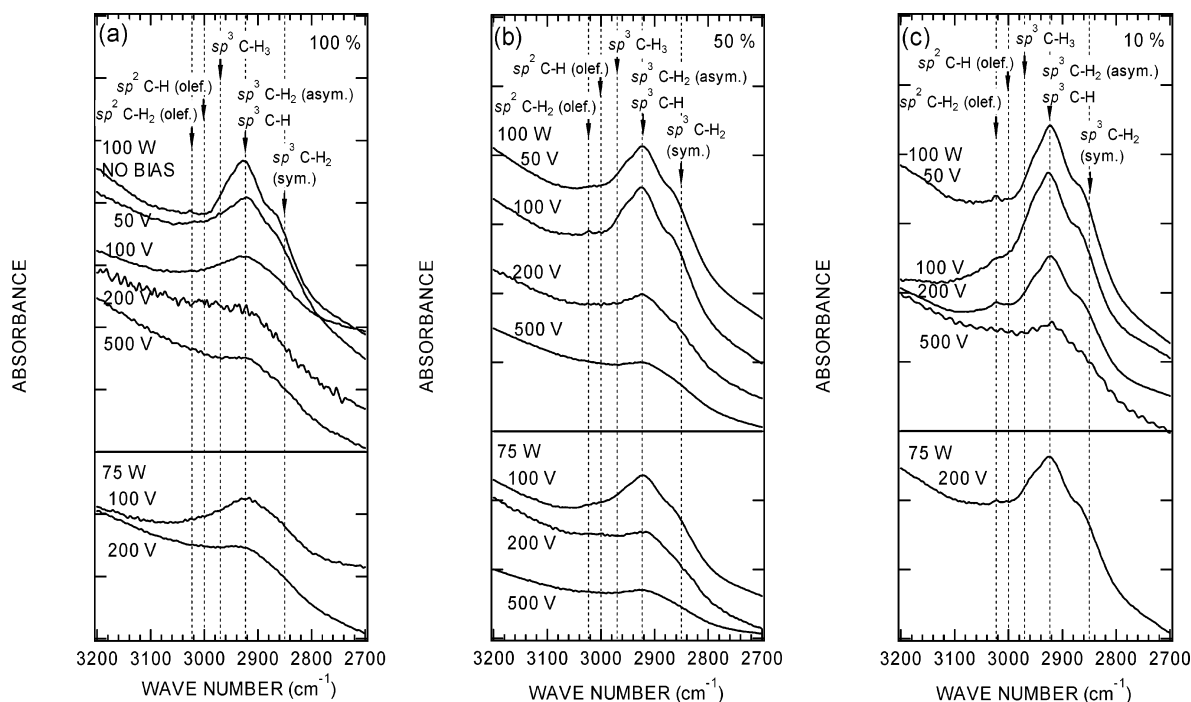


**Figure 4.** IR absorption spectra of the films deposited with various  $V_s$  at  $P = 75$  and  $100$  W and  $R_d =$  (a) 100%, (b) 50%, and (c) 10%. One division in the vertical axis corresponds to 0.05 in absorbance.

technique is effective for stress reduction without a significant degradation of hardness of  $a$ -C:H films. When  $R_d$  was reduced from 100% to 50% with  $V_s = 200$  V and  $P = 100$  W, the stress decreased more rapidly by 63% from 2.5 to 0.93 GPa than the hardness by 32% from 25 to 17 GPa. It was found that the relatively low stress of 0.6 GPa was obtained with  $P = 75$  W,  $V_s = 200$  V and  $R_d = 50\%$  for the films with the hardness of 15 GPa. In the case of  $R_d = 10\%$  the soft films were formed with the hardness less than 10 GPa.

Thus we investigated the tribological properties of the film prepared with  $R_d = 50\%$ ,  $V_s = 200$  and  $P = 75$  W, which had the low stress of 0.6 GPa without a degradation of hardness as mentioned above. Figure 6 shows the dependence of the specific wear rate on the testing cycle and load for the film deposited

with the conditions of  $V_s = 200$  V,  $R_d = 50\%$  and  $P = 75$  W for 120 min. The film thickness was 2.0  $\mu\text{m}$ . The film could endure for the load of 20 N and 20 000 cycles without adhesion failure. For 1000 cycles test, the specific wear rate decreased from  $7.8 \times 10^{-7}$  to  $4.9 \times 10^{-8}$   $\text{mm}^3/\text{Nm}$  with increasing load from 1 to 20 N. The specific wear rate increased by a factor of 2.6 when the cycle was raised from 1000 to 20 000. The friction coefficient decreased from 0.09 to 0.04 with increasing load from 1 to 20 N after the 20 000 cycle test. It is concluded that in terms of the specific wear rate and the lifetime the deposition condition of  $a$ -C:H was optimized at  $R_d = 50\%$ ,  $V_s = 200$  V, and  $P = 75$  W in the present study. The improved tribological properties might result from the following effects: (1) the reduced stress suppressed delamination failure on the tribological



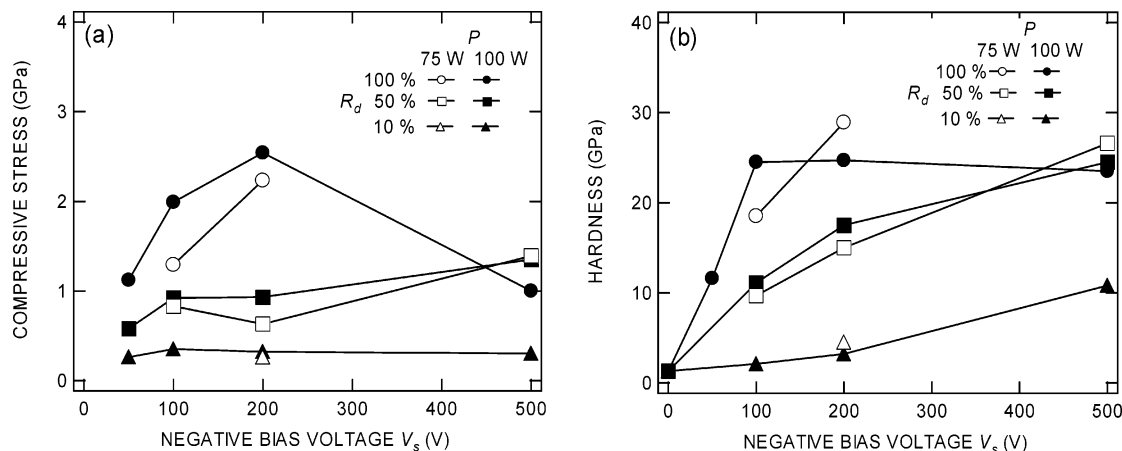


Figure 5. (a) Compressive stress and (b) hardness of the films deposited with various  $V_s$  and  $R_d$ .

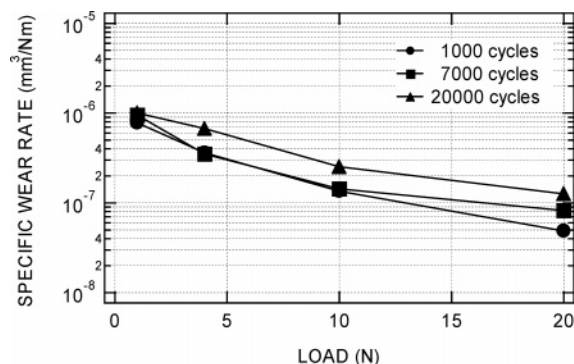


Figure 6. Load and sliding time dependence of the specific wear rate of the film deposited with  $P = 75$  W,  $V_s = 200$  V, and  $R_d = 50\%$  for 120 min.

test; (2) the increased thickness up to 2  $\mu\text{m}$  prevented the propagation of the stress, which was caused by the ball, to the interface, leading to the suppression of the delamination failure.

It should be noted that  $V_s$  of 100 V was relatively high for the films with the hardness of 25 GPa. This  $V_s$  value is approximately 1/9 of the value for the results using benzene,<sup>20</sup> which is as heavy a molecular as toluene, and comparable with that for methane.<sup>21</sup> It is considered that this results from the high ion flux of the highly fragmented carbon species due to the high-density plasma and/or from the collisionless acceleration of the ion in the sheath due to the low working pressure, demonstrating one of the advantages of the present method.

**3.2.3. Uniformity on Three-Dimensional Coating.** Using the deposition conditions ( $P = 75$  W,  $V_s = 200$  V,  $R_d = 50\%$ ) found in the previous section, three-dimensional coating was performed using the  $\phi$  60 mm  $\times$  80 mm hexagonal substrate holder (Figure 7a). Figure 7b shows the thickness variation of the deposited films. The averaged thickness was 2.0  $\mu\text{m}$ , and the variation was within  $\pm 3.5\%$  in the azimuthal direction. The thickness of the sample deposited on the top of the holder was higher than the samples on the sidewalls by 2%. Figure 7c shows the variation in refractive index of the samples. The refractive index ( $n$ ) was 2.1 with the variation less than  $\pm 1\%$ . These results clearly demonstrate that the present method is effective for uniform three-dimensional coating of  $a$ -C:H.

#### 4. Conclusions

A new deposition technique has been developed for volumetric three-dimensional coating of amorphous hydrogenated carbon via low-pressure inductively coupled plasma enhanced chemical vapor deposition using multiple low-inductance an-

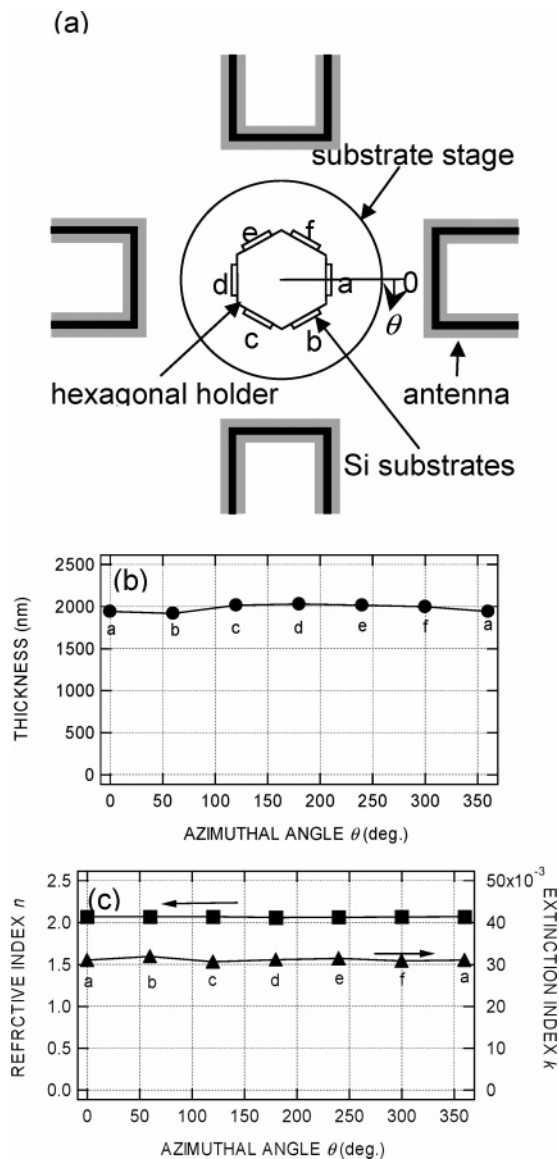


Figure 7. (a) Setup of the substrates on the  $\phi$  60  $\times$  80 mm hexagonal holder for three-dimensional coating. Variations of film (b) thickness and (c) refractive index of the films deposited with  $P = 75$  W,  $V_s = 200$  V, and  $R_d = 50\%$  for 120 min.

tenna system. The uniformity of the plasma density is  $\pm 5\%$  within lateral  $\phi$  200 mm and  $\pm 10\%$  in the axial height of 100 mm for argon plasma with the pressure of 0.1 Pa and the total

RF power input as low as 400 W ( $P = 100$  W). Thick (2.0 microns) amorphous hydrogenated carbon films with the thickness uniformity of  $\pm 3.5\%$  and the refractive index uniformity of  $\pm 1\%$  have been successfully deposited on the substrates placed on the six side walls and the top of the  $\phi$  60 mm  $\times$  80 mm hexagonal substrate holder in the pure toluene plasma with the pressure as low as 0.04 Pa and the total RF power input as low as 300 W ( $P = 75$  W). It is also found that precisely controlled ion bombardment by the pulse biasing led to the explicit observation in Raman and IR spectra of the transition from the polymer-like structure to the DLC structure accompanied by dehydrogenation due to ion bombardment. In addition, using pulse biasing technique, the reduced compressive stress of 0.6 GPa without a significant degradation of the hardness (15 GPa) has been achieved. The 2.0  $\mu$ m thick films are durable for the tribology test with a high load of 20 N up to more than 20 000 cycles, showing the specific wear rate and the friction coefficient were  $1.2 \times 10^{-7}$  mm<sup>3</sup>/Nm and 0.04, respectively.

## References and Notes

- (1) Grill, A.; Patel, V.; Meyerson, B. S. In *Application of Diamond Films and Related Materials*; Tzeng, Y., Yoshikawa, M., Feldman, A., Eds.; Elsevier Science: New York, 1991.
- (2) Erdemir, A.; Switala, M.; Wei, R.; Wilbur, P. *Surf. Coat. Technol.* **1991**, 50, 17.
- (3) Erdemir, A.; Eryilmaz, O. L.; Fenske, G. *J. Vac. Sci. Technol. A* **2000**, 18, 1987.
- (4) Fontaine, J.; Donnet, C.; Grill, A.; LeMogne, T. *Surf. Coat. Technol.* **2001**, 146/147, 286.
- (5) Grill, A. *Surf. Coat. Technol.* **1997**, 94/95, 507.
- (6) Malaczynski, G. W.; Hamdi, A. H.; Elmoursi, A. A.; Qui, X. *Surf. Coat. Technol.* **1997**, 93, 280.
- (7) Watanabe, T.; Yamamoto, K.; Koga, Y.; Tanaka, A. *Jpn. J. Appl. Phys.* **2001**, 40, 4684.
- (8) Watanabe, T.; Yamamoto, K.; Koga, Y.; Tanaka, A. *Sci. Technol. Adv. Mater.* **2001**, 2, 539.
- (9) Watanabe, T.; Yamamoto, K.; Tsuda, O.; Tanaka, A.; Koga, Y. *Jpn. J. Appl. Phys.* **2002**, 41, 6165.
- (10) Watanabe, T.; Yamamoto, K.; Tsuda, O.; Tanaka, A.; Koga, Y.; Takai, O. *Diam. Relat. Mater.* **2003**, 12, 2083.
- (11) Watanabe, T.; Ishihara, M.; Yamamoto, K.; Tsuda, O.; Tanaka, A.; Koga, Y.; Takai, O. *Diam. Relat. Mater.* **2003**, 12, 105.
- (12) Watanabe, T.; Yamashita, N.; Suzuki, M.; Ishihara, M.; Ohana, T.; Yamamoto, K.; Tsuda, O.; Tanaka, A.; Koga, Y. *New Diam. Frontier Carbon Technol.* **2004**, 14, 161.
- (13) Setsuhara, Y.; Shoji, T.; Ebe, A.; Baba, S.; Yamamoto, N.; Takahashi, K.; Ono, L.; Miyake, S. *Surf. Coat. Technol.* **2003**, 174/175, 33.
- (14) Yoshikawa, M.; Katagiri, G.; Ishida, H.; Ishitani, A.; Akamatsu, T. *J. Appl. Phys.* **1988**, 64, 6464.
- (15) Tamor, M. A.; Vassel, W. C. *J. Appl. Phys.* **1994**, 76, 3823.
- (16) Robertson, J. *Diam. Relat. Mater.* **1993**, 2, 984.
- (17) The ion range was calculated with the parameters described in ref 16 using the TRIM code (Biersack, J. P.; Haggmark, L. G. *Nucl. Instrum. Methods* **1980**, 174, 257).
- (18) Couderc, P.; Catherine, Y. *Thin Solid Films* **1987**, 146, 93.
- (19) Nagai, I.; Ishitani, A.; Kuroda, H.; Yoshikawa, M.; Nagai, N. *J. Appl. Phys.* **1990**, 67, 2890.
- (20) Koidl, P.; Wagner, C.; Dischler, B.; Wagner, J.; Ramsteiner, M. *Mater. Sci. Forum* **1990**, 52, 41.
- (21) Jiang, X.; Zou, J. W.; Reichelt, K.; Grunberg, P. *J. Appl. Phys.* **1989**, 66, 4729.